INTERMEDIATE-VELOCITY CLOUDS APPROACHING THE GALACTIC PLANE

by

MATTHEW CHARLES PARKER

(Under the Direction of Robin L. Shelton)

ABSTRACT

Based on their negative velocities and the orientations of their cometary tails, many intermediate-velocity clouds (IVCs) appear to be falling into the Milky Way's disk. In order to investigate the past and future evolution of these clouds, we have performed a suite of hydrodynamical simulations, two of which are presented here. Our simulations are designed to model IVC 86-36 in the Pegasus-Pisces Arch. In all of the simulations, the clouds develop long tails as they pass through the low-density thick disk and dissipate when they enter the higher density gas within ~ 300 pc of the midplane.

INDEX WORDS: Galaxy: general --- Hydrodynamics --- ISM: clouds --- ISM: kinematics and dynamics --- Methods: data analysis

INTERMEDIATE-VELOCITY CLOUDS APPROACHING THE GALACTIC PLANE

by

MATTHEW CHARLES PARKER

B.S., Francis Marion University, 2008

M.A., Western Governors University, 2013

A Thesis Submitted to the Graduate Faculty of The University of Georgia in Partial Fulfillment of the Requirements for the Degree

MASTER OF SCIENCE

ATHENS, GEORGIA

2019

INTERMEDIATE-VELOCITY CLOUDS APPROACHING THE GALACTIC PLANE

by

MATTHEW CHARLES PARKER

Major Professor:	Robin L. Shelton
Committee:	Loris Magnani
	Jean-Pierre Caillault

Electronic Version Approved:

Suzanne Barbour
Dean of the Graduate School
The University of Georgia
August 2019

ACKNOWLEDGEMENTS

I would like to express my deepest appreciation to my mentor, Dr. Robin Shelton, for her continued support and guidance. The insight she provided was invaluable in both my education and research.

Many thanks go to Dr. Jason Galyardt for his expertise and guidance in developing and running hydrodynamical simulations that were invaluable to my research.

Chapter 2 of this thesis is based on a publication in which I had the pleasure of collaborating with Dr. Yasuo Fukui and Dr. Kengo Tachihara. I truly appreciate the data they provided as well as the feedback and suggestions that helped shape the final article.

I would like to thank the other two members in my advisory committee, Dr. Loris Magnani and Dr. Jean-Pierre Caillault, for being outstanding professors and advisors.

I would also like to thank my wife, Lauren, and our dog, Linus, for their endless love and motivation. Without their mental and emotional support, this whole endeavor would have been an even tougher challenge.

TABLE OF CONTENTS

Page

LIST OF TABLES

Page

LIST OF FIGURES

Page

CHAPTER 1

INTRODUCTION

1.1 INTERMEDIATE-VELOCITY CLOUDS

Throughout the Milky Way Galaxy there are clumps of interstellar gas and dust that are moving with local standard of rest (LSR) speeds between 20 and 100 km s^{-1}. In other words, this is the speed the gas and dust are moving relative to our solar system. These clumps are called intermediate-velocity clouds (IVCs) because they have velocities between those generally accepted for High-Velocity Clouds (HVCs), whose speeds exceed ~100 km s^{-1}, and Low-Velocity Clouds (LVCs), whose speeds are below ~20 km s^{-1}. A large number of IVCs are located in the lower galactic halo (a spherical portion of the galaxy that surrounds the more visible galactic disk) and have negative velocities, which indicates they are falling towards the galactic plane.

As these clouds approach the galactic midplane, they interact with material in the interstellar medium (ISM), which is the matter that exists in the space between star systems. This interaction sweeps material back behind the main portion of the cloud forming a tail similar to the morphology of comets. This head-tail configuration helps show the direction the IVC is moving since the tail will tend to point away from the direction of motion. Therefore, if the cloud is falling towards the galactic midplane, the head will be on the side of the cloud approaching the galactic plane while the tail will be pointing away from the plane.

According to Albert & Danly (2004), the origins of IVCs is still a topic of discussion but the main theories include the Extragalactic Infall Model and the Galactic Fountain Model. The Extragalactic Infall Model proposes the clouds were formed outside of our Galaxy and have fallen into it. For example, IVCs could be gas that was stripped from nearby galaxies and is falling into our galaxy. The Galactic Fountain Model suggests the clouds are composed of gas and dust that was once a part of our Galactic midplane but was ejected by means of supernovae explosions. After being ejected, the gas and dust cools and condenses, forming IVCs that are or will eventually be falling back towards the midplane of our galaxy.

These IVCs are generally observed using the 21 cm emission line from a neutral hydrogen (HI) atom. Each of those photons is a microwave with a wavelength of 21 cm that was created when the electron of a neutral hydrogen atom underwent a change in energy state. This change is called a spin-flip transition and the emission is detected using radio telescopes. Since hydrogen is the most abundant element in the ISM, HI is used to map out the entire Galaxy. Using the Doppler shift of the 21 cm wavelength microwave emitted by HI, the radial velocities of clouds are determined. Radial velocity is the speed of an object moving towards or away from the observer. Another method for detecting IVCs is the utilization of stars behind the clouds. By using a star whose distance and spectrum are known, if the cloud is between the observer and the star, absorption lines from trace elements will be present allowing for optical and ultraviolet observations of the clouds.

According to Kuntz & Danly (1996), the northern hemisphere consists of several IV complexes including the Intermediate-Velocity Arch (IV Arch), the Intermediate-

Velocity Spur (IV Spur), and the Low-Latitude IV Arch (LLIV Arch). The southern hemisphere contains IV complexes like the Pegasus-Pisces Arch and complex gp (Wakker (2001)). In both hemispheres, the IV complexes primarily have negative velocities indicating they are on a trajectory toward the midplane of the galaxy.

Determining the distance to an IVC is no small task, but it is crucial for providing insight into the origin of the cloud and other properties of the IVC including size, mass, density, etc. Limits on the distances to IVCs can be placed on the clouds using the absorption lines from stars that lie along the same line-of-sight as the cloud. Line-of-sight (LOS) refers to the straight-line path from the observer in the direction they are looking. If absorption lines are detected, the cloud is in front of the star and an upper limit can be placed on the distance to the cloud that is similar to the known distance of the star. If no absorption lines are detected, the cloud is behind the star and a lower limit can be placed on the distance to the cloud. Although this technique is helpful, the location of clouds is often weakly constrained to a wide range of potential distances. For example, Kuntz & Danly (1996) placed the IV Arch, which is the largest intermediate-velocity feature in the galaxy, at a distance between 800 and 1500 parsecs (pc) above the galactic plane and the IV Spur at a height between 0.23 and 2.1 kpc. As you will see in Chapter 2, IVC 86-36, which is the IVC of interest, is also weakly constrained to be at a distance between 0.2 and 3 kpc. To put these distances into context, one parsec is equivalent to 3.086×10^{13} km or 3.26 light-years.

In general, it appears HVCs are more distant than IVCs. This may be an indication that IVCs were once a part of HVCs and have since decelerated due to drag as they approach the galactic disk. However, IVCs, in general, have been found to have

metallicities higher than that of HVCs. In astronomy, any element heavier than hydrogen or helium is considered a metal, so metallicity is an indication of the abundance of these elements. The metallicity of the Sun is used as the standard, so an object with an abundance of 0.5 solar has half the metallicity of the Sun, an object with a metallicity of 0.1 solar has one-tenth the abundance of the Sun, and so on. For example, Richter et al. (2001) determined the IV Arch has a near-solar abundance, while Fitzpatrick & Spitzer (1997) observed components of the Pegasus-Pisces Arch to have an abundance of 0.5 solar.

Since IVCs tend to have negative velocities and near-solar metallicities, it would seem to suggest IVCs originated within the Galactic plane. If this is the case, the Galactic Fountain Model may be the strongest contender for the method by which IVCs originated. However, another possibility is that mixing is occurring between the cloud and the ambient material, which is raising the metallicity of the cloud to near-solar. Also, there are examples of IVCs with sub-solar metallicities such as IV21 (Hernandez et al. (2013)). It does not seem likely that these clouds originated within the Galactic disk and may fit more closely with the predictions given by the Extragalactic Infall Model. Therefore, more than one explanation may be required to identify the origin of intermediate-velocity clouds.

1.2 SIMULATING IVC 86-36

In Chapter 2, we will discuss further IVC 86-36, whose name identifies its Galactic coordinates as being $(l, b) = (86^{\circ},-36^{\circ})$. Galactic longitude ($l$) is an angle measured by an observer looking from Earth toward the Galactic center and sweeping

counter-clockwise across the Galactic equator, and Galactic latitude (*b*) is the angle measured starting at the Galactic midplane and moving above or below it from the viewpoint of the Earth. A positive latitude indicates a position north of the Galactic midplane, while a negative latitude indicates a position south of the Galactic midplane. IVC 86-36 is located to the south of the Galactic midplane in the area of the Pegasus-Pisces Arch.

IVC 86-36 was observed by our collaborators Fukui et al. (2018) and its head was determined to have an angular size of ~5°. This is the angle subtended by the cloud in the sky, but it does not give the actual size of the cloud. In order to determine the size of the cloud, the distance to the cloud must be known. As discussed early, attempts to determine the distances to IVCs often results in a wide range of potential distances. This is the case for IVC 86-36, so the actual size of the cloud cannot be narrowed down. Using the Galactic latitude, Fukui et al. (2018) calculate the actual length of the cloud using $L=0.66d$, where d is the distance to the cloud expressed in kpc. Since the cloud is within a wide range of possible distances, the length of the cloud is also weakly constrained to be between 0.13 and 2 kpc.

A property of the cloud that has been measured is its column density, which was determined to be of 2×10^{20} cm^{-2}. The column density is a measure of the number of neutral hydrogen (HI) atoms per square centimeter (cm^2). In other words, it is the amount of HI between the observer and the object being observed along a line-of-sight with an area of 1 cm^2. Fukui et al. (2018) also estimated the mass of the head of the cloud to be $7\times10^3(d/1\text{kpc})^2$ $M_\odot$, where d is the distance to the cloud. This calculation places the

mass for the head of IVC 86-36 to be between 260 $M_{\odot}$ and 70,000 $M_{\odot}$ at distances between 200 pc and 3 kpc.

Another measurable property of IVCs is velocity dispersion, which is the square root of the variance of the velocity field for an object. After determining the radial velocities along numerous lines-of-sight, the mean velocity of an object can be determined and the difference between the velocity along a line-of-sight and the mean velocity can be determined. A portion of the velocity dispersion is due to thermal broadening, which is a change in the speed of particles due to a change in temperature. As temperature increases, the speed of the particles also increases and a decrease in temperature decreases the speed of the particles. Therefore, a cloud with a higher temperature will tend to have greater velocity dispersion.

Using the known properties of IVC 86-36, we design and perform hydrodynamical simulations to model this intermediate-velocity cloud. Our hydrodynamical simulations are those that model the fluid dynamics of the material in our Galaxy. In other words, the interactions between gas and dust in the Milky Way can be investigated as they flow past one another. Therefore, the evolution of an IVC moving through interstellar material can be studied. These simulations take into account the density and gravity throughout the Galaxy. Since the Milky Way is a spiral galaxy, its densest region is within the thin disk, which has a radius of ~25 – 30 kpc and a thickness of ~0.5 kpc. This density is greatest at the Galactic center and decreases as you move out toward the edge. It also decreases moving north and south from the Galactic midplane. Therefore, the simulations must take into account where in the Galaxy we place the simulated IVC in order for it to most closely match IVC 86-36. To do this, we place the

simulated IVC in the general vicinity of the Solar System, which is ~8 kpc from the Galactic center. In the following chapter, further discussion of IVC 86-36 and the results of our simulations will be examined.

CHAPTER 2

EVOLUTION OF INTERMEDIATE-VELOCITY CLOUDS ON COLLISION COURSES WITH THE GALACTIC PLANE: THE EXAMPLE OF IVC 86-36

2.1 INTRODUCTION

Throughout the Milky Way, Intermediate-Velocity Clouds (IVCs) are speeding through interstellar space as they plunge toward the disk. Evidence of their approach toward the midplane can be seen in the way the clouds tend to form predictable features similar to the morphology of comets. In other words, a long tail forms behind the head of the cloud preferentially oriented away from the disk (Brüns et al. (2000); Brüns & Mebold (2004); Peek et al. (2007)). According to Fukui et al. (2018), the Pegasus-Pisces Arch contains several of these IVCs with elongated shapes. Additionally, the majority of IVCs have negative velocities, which also indicates that they are generally falling toward the disk. IVCs move with local standard of rest (LSR) speeds, |v|, between 20 - 100 km/s (Albert & Danly (2004)).

Intermediate-velocity clouds also tend to be located in the lower Galactic halo, within ~ 2 kpc above the disk (Röhser et al. (2016)). For example, the Intermediate-Velocity Arch (IV Arch), which is the largest IV feature, is located at a height above the Galactic plane between 0.8 and 1.5 kpc (Kuntz & Danly (1996)).

The main techniques used to study IVCs include detecting the 21 cm emission from neutral hydrogen gas and detecting the absorption of optical and ultraviolet light by

trace elements at the necessary velocities in the spectra of distant stars (Albert & Danly (2004)). However, there are the rare molecular IVCs (MIVCs) located several hundred parsecs above the disk that also contain a high enough molecular gas column density to be detected using carbon monoxide ^{12}CO(1→0) emission (Magnani & Smith (2010)).

The origin of IVCs is debated. According to Albert & Danly (2004), the dominant models include the Galactic Fountain model, which states that the material had originally been blown out of the disk before eventually falling back towards the disk, and the Extragalactic Infall model, which describes IVCs as having come from outside of our Galaxy. The metallicity of IVCs is one strand of evidence that may point toward their origin. An IVC with a solar abundance that is similar to that of material in the vicinity of the sun could indicate an origin from within the galactic disk similar to that described by the Galactic Fountain model, while an IVC with a metallicity much less than that of the solar neighborhood may point towards an origin from outside the Galaxy similar to that described by the Extragalactic Infall model (See Albert & Danly (2004) and references therein). Additionally, sub-solar IVCs could possibly have originated from the outer Galactic disk due to fountain model-behavior, and near-solar metallicity IVCs could have originated outside the Galaxy and have had their metallicity boosted by mixing with galactic gas.

According to Röhser et al. (2016), neutral IVCs consist of near solar metallicity gas. Several IVCs including the IV Arch have near-solar abundances, which suggests they could consist predominantly of recycled disk material. Based on absorption-line measurements, most of the large northern IVCs have a relatively high metallicity ranging between 0.5 and 1.0 solar (Wakker (2001); Richter et al. (2001)). According to Albert &

Danly (2004), evidence is mounting in favor of at least some IVCs having the return flow of a Galactic fountain.

However, there is evidence for the existence of IVCs with sub-solar abundance, which indicates an origin outside of the Galaxy. IV21 is a low-metallicity MIVC with an abundance of ~ 0.4 solar and is located at a height of ~ 300 pc above the disk (Hernandez et al. (2013)). Clouds with sub-solar abundances may be falling from outside the Milky Way, material stripped from nearby galaxies (Wakker & van Woerden (1997); Blitz et al. (1999); Lockman et al. (2002); Connors et al. (2006)), or fountain material that originated in the outer Galaxy.

IVC 86-36, in the Pegasus-Pisces Arch (Fukui et al. (2018)), is one such example of a low metallicity IVC that appears to be approaching the Galactic disk. It has been well studied and has an elongated distribution and a column density of 2×10^{20} cm^{-2}. Here, we present simulational models of IVC 86-36 that were chosen from a larger suite of simulations because they best match the observed characteristics of the cloud. The simulations continue on in simulational time, showing that the cloud's fate is to disperse when it comes within ~ 300 pc of the Galactic midplane.

In this article, simulational models of IVCs falling into the Galactic disk will be analyzed and compared to the data for IVC 86-36. Section 2 discusses the IVC observed by Fukui et al. (2018) and the simulations used to model clouds falling into the Galactic disk. The results are presented in Section 3 where figures showing the evolution of the simulated IVCs can be seen. We also discuss the comparison of our simulated IVCs to IVC 86-36 using several strands of evidence, such as physical features, line-of-sight

velocity, velocity dispersion, and HI 21 cm intensity. A summary of the findings is presented in Section 4.

2.2 METHODS

2.2.1 Observed Cloud

Fukui et al. (2018) observed an intermediate-velocity cloud (IVC 86-36) located at (l, b) = (86°,−36°) in the Pegasus-Pisces Arch using HI 21 cm emission obtained by GALFA with the Arecibo telescope using an angular resolution of 4'.

IVC 86-36 is detected with a range of radial velocities between −60 km s^{-1} and −20 km s^{-1} and is falling with a line of sight velocity of ~ 60 km s^{-1} at an angle of ~ 45° towards the Galactic disk, as seen in Figure 4. This angle is estimated using the distances spanned in both the Galactic latitude and Galactic longitude and assuming that the cloud is straight and falling perpendicular to our line of sight. Based on optical spectroscopy using the absorption of background stars, the observed cloud is determined to be at a distance within ~ 3 kpc having a head with an angular size of ~ 5° (i.e., ~ 300′) (Fukui et al. (2018)).

The star HD215733 is located behind the head of IVC 86-36. Based on spectral type of B1 II, V=7.3, E(B-V)=0.10, and M_V=−5.3 of HD215733 (Walborn (1976); Mermilliod (1987); Fitzgerald (1970); Lesh (1968)), the star is estimated to be at a distance of 2900 pc. According to Fukui et al. (2018), GAIA estimates the measured distance to HD215733 to be ~ 3.5 kpc, which limits the distance to the cloud to be less than the distance to the star. Another background star, PG0039+049, is also used. It is located in part of the tail of IVC 86-36 and using optical absorption, the distance is

estimated to be less than 1050 pc (Wakker (2001)). For simplicity, the tail of IVC 86-36 is assumed to be at the same distance from the sun as the head. Using Galactic latitude, the actual length of IVC 86-36 is calculated using the equation L=0.66*d*, in which *d* is the distance to the cloud in parsecs. To give a sense of scale, for distances between 200 pc and 3 kpc, the length of the cloud is between 130 pc and 2 kpc, respectively. If IVC 86-36 were to be at a height below the disk of 1 kpc with an upward velocity of ~ 60 km s^{-1} at an angle of ~ 45°, the timescale for IVC 86-36 to collide with the Galactic disk is estimated to be ~20 Myrs.

According to Fukui et al., the mass of the HI and He in the head of IVC 86-36 is estimated to be $7\times10^{3}(d/1\text{kpc})^{2}$ $M_{\odot}$; therefore, the mass range is between 260 $M_{\odot}$ and 7×10^{4} $M_{\odot}$ for distances between 200 pc and 3 kpc. Even with an HI column density of 2×10^{20} cm^{-2}, the dust emission of the IVC is not detectable indicating a metallicity of less than ~ 0.2 solar abundance. In other words, the dust optical depth of IVC 86-36 appears to be less than one-fifth that of the ISM in the solar surroundings. Fukui et al. interpret this to indicate the cloud did not originate in the Galactic disk by means of the Galactic Fountain Model. According to Fukui et al. (2018), the location of IVC 86-36 in the southern sky may indicate an origin in the Magellanic system, which shares a similar metallicity between 0.1 - 0.2 solar (D'Onghia & Fox (2016)). Additionally, Fukui et al. (2017) and Tsuge et al. (2019) present analyses of the Planck dust emission in the Large Magellanic Cloud (LMC) and argue that part of the gas in the galaxy has significantly lower metallicity due to tidal interaction with the low metallicity Small Magellanic Cloud (SMC).

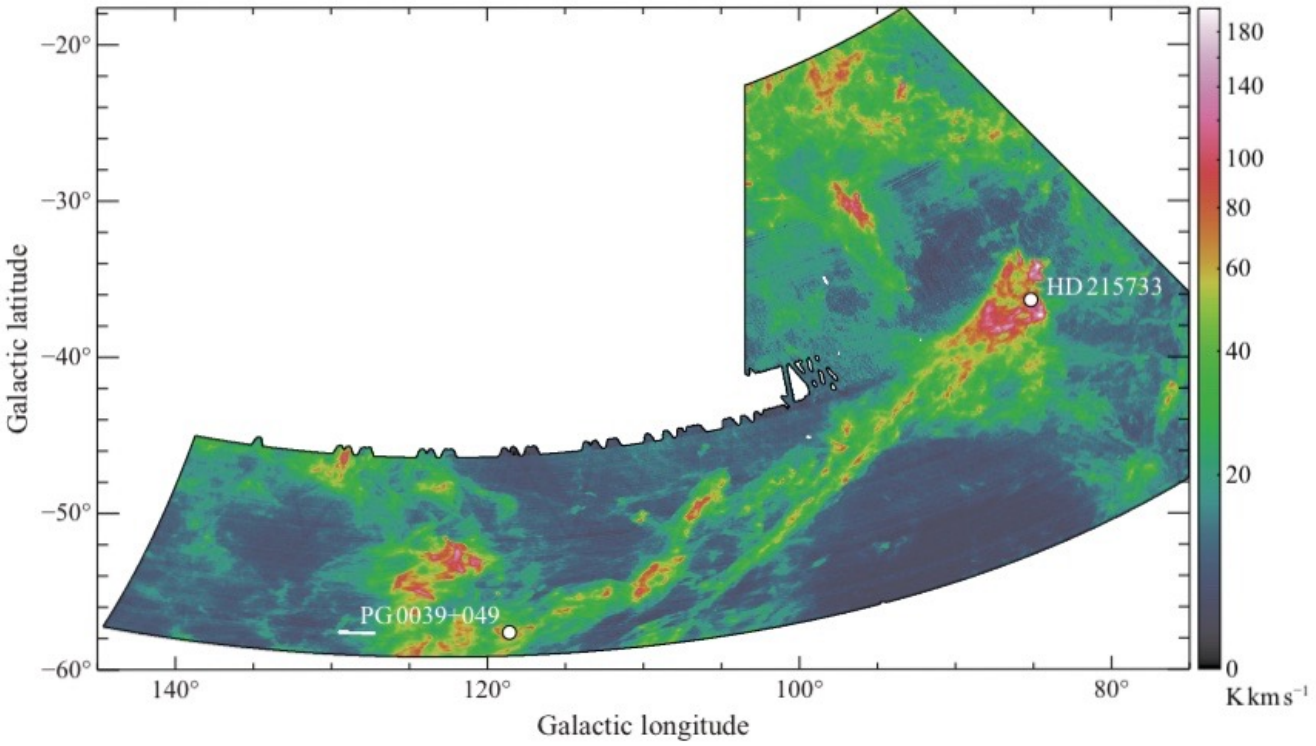

Figure 1. IVC 86-36 observed by Fukui et al. (2018) plotted with intensity in units of K km s^{-1}. In this figure, the galactic midplane (not shown) would be horizontal at a galactic latitude of 0°, and the IVC is at an angle of $\sim 45°$ with respect to it.

2.2.2 Simulations

To model the hydrodynamics of a cloud like IVC 86-36 falling toward the Galactic disk, we are using the simulation package FLASH version 4.3 in three dimensions with a Cartesian coordinate system. Since the distance to IVC 86-36 is not known precisely, we modeled two clouds, IVC 1 and IVC 2, each at a different distance from the Earth. The observed location of the head of IVC 86-36, at ~ 40° below the Galactic plane, placed a constraint on the simulation setups, such that any adjustment to the assumed distance to the cloud also required an adjustment to the initial height of the cloud. When we simulated the cloud as being 200 pc from Earth (i.e., IVC 1), we started it 1.1 kpc from the midplane, and when we simulated it as being 3 kpc from the Earth (i.e., IVC 2), we started it 2.0 kpc from the midplane. At the beginning of each simulation, the cloud is spherical and has a radius and hydrogen number density that agree with IVC 86-36's present angular size and column density of 2.0×10^{20} cm^{-2} that were measured from observation. For instance, IVC 1 has an initial radius of 43.7 pc and an initial hydrogen number density of 0.84 cm^{-3}, while IVC 2 has an initial radius of 87.3 pc and an initial hydrogen number density of 0.43 cm^{-3}. The values used for each run can be seen in Table 1.

Initially, we make each cloud spherical and, within the cloud, the density and temperature follow a smooth transition from the center of the cloud to its outer edge as discussed in Galyardt & Shelton (2016). The conditions in the cloud are set such that the cloud is initially in pressure balance with the ambient medium. The halo material around the Galactic disk is also in hydrostatic equilibrium with a smooth pressure gradient from

Table 1. Simulated IVCs: Initial Parameters

Parameter	IVC 1	IVC 2
Column Density	2.0×10^{20} cm^{-2}	2.0×10^{20} cm^{-2}
Hydrogen Number Density	0.84 cm^{-3}	0.43 cm^{-3}
Cloud Radius	43.7 pc	87.3 pc
Cloud Mass	$\sim$ 7300 M$_\odot$	$\sim 2.9\times10^{4}$ M$_\odot$
Angle Relative to the Disk	45°	45°
Total Velocity in xz-Plane	-99 km s^{-1}	-99 km s^{-1}
Height above Disk	1.100 kpc	2.000 kpc

NOTE—For each simulated IVC, the cloud is initially moving at a 45° angle relative to the disk with a velocity in the x-direction of 70 km s^{-1} and a velocity in the z-direction of -70 km s^{-1} giving a resultant velocity of ~ -99 km s^{-1}.

the center of the Galactic disk out past the edges of our domain. The gravitational strength and thermal pressure in use are the same as those in Galyardt & Shelton (2016) for a cloud at a galactocentric radius of 10 kpc, which is roughly similar to that of the solar system. This hydrostatic equilibrium is not completely stable at our size range, which can be seen in the figures as a small pressure wave moving within the domain. However, it does not appear that this pressure wave has any significant impact on the evolution of our IVCs. The clouds are assigned 0.1 solar metallicities, while the ambient medium is assigned a metallicity of 0.3 solar.

The simulations are performed in the reference frame of the Galaxy. Each cloud has an initial overall velocity of $\sim$ 100 km s^{-1} directed at a 45° angle in the *xz*-plane of the domain. We started with this higher velocity to allow for deceleration due to drag so when the cloud reaches its current distance its line-of-sight velocity will be similar to that of IVC 86-36.

Since our clouds are moving at a 45° angle relative to the disk, modeling clouds at various distances from the Sun requires a different domain size for each simulation in

order to visualize the collision of the cloud with the disk while also minimizing resources used and computational run time. When the size of the domain increases, the number of processors used in the calculations and the amount of time it takes for the simulation to run are also increased. This is needed to maintain high resolution.

Simulations with greater initial cloud heights require domains that are both taller and wider. For IVC 1, whose cloud has an initial height above the disk of 1100 pc, the domain size is 1088 pc in the *x*-direction by 128 pc in the *y*-direction by 1600 pc in the *z*-direction and the maximum number of cells is 544 × 64 × 800 cells. As seen in Figure 2(a), the center of our cloud is located at a *z*-height of 1100 pc and the Galactic disk is at the origin on the *z*-axis and spans the entire length of the *x*-axis. The *z*-axis continues above the center of the Galactic disk for ~ 400 pc in order to observe the condition of the cloud as it passes through the entire disk. For IVC 2, whose cloud has an initial height above the disk of 2000 pc, the domain size is expanded to 2336 pc × 192 pc × 2592 pc and the maximum number of cells increases to 1168 × 96 × 1296 cells. The increase in the *y*-direction is needed to account for the increase in the cloud's radius. Each run has a final cell size of 2 pc × 2 pc × 2 pc after refinement.

2.3 RESULTS

2.3.1 Physical Features

The evolution of the simulated clouds in IVCs 1 and 2 can be seen in Figures 2 and 3, respectively. As discussed earlier, they both start with a spherical cloud falling towards the Galactic midplane. Similar to those seen in the HVC models by Heitsch & Putman (2009), our IVCs also develop tails. As seen in Figures 2 and 3, an IVC

interacting with interstellar material will form a tail pointing away from the direction of motion, much like a comet's morphology. This is also seen with observed clouds, such as IVC 86-36 (Figure 1). Comparing the simulated clouds (Figures 2 and 3) to IVC 86-36, we see that their structures are similar in several ways. They both form a head followed by a long, straight tail. Additionally, much of the tail is straight with a winding structure at the end. IVC 86-36 also has a tail made up of two identifiable filamentary streamers. Although this is not seen in IVC 1, which has a smaller radius and began closer to the disk, it looks like it may be starting to form in IVC 2. Additionally, we have also seen this feature in several of our previous simulations.

Another feature of IVC 86-36 is the asymmetry of its head. The side of the cloud that is closest to the Galactic midplane is flatter and smoother than the side facing away from the midplane, which looks to be rougher and rounder. Although this is not noticeable in IVC 1, IVC 2 begins experiencing a similar flattening of its head at around the time it reaches ~ 300 pc above the Galactic midplane as seen in Figure 3(f).

Upon closer inspection of Figures 2(b) and 3(b), it can be seen that the simulated IVCs develop bow shocks that surround their heads. These bow shocks protect the main portion of each cloud allowing it to retain a roundish shape even as the cloud passes through hundreds of parsecs of material. Conversely, these bow shocks are not seen in models of HVCs that evolve at much greater heights above the Galactic disk, such as those by Gritton et al. (2014). This could be a major factor in the difference between the evolution of IVCs and HVCs. It is possible that IVC 86-36 has also been protected by a bow shock as it passes through interstellar material, but the density contrast in such a shock would likely make it difficult to observe in HI emission images.

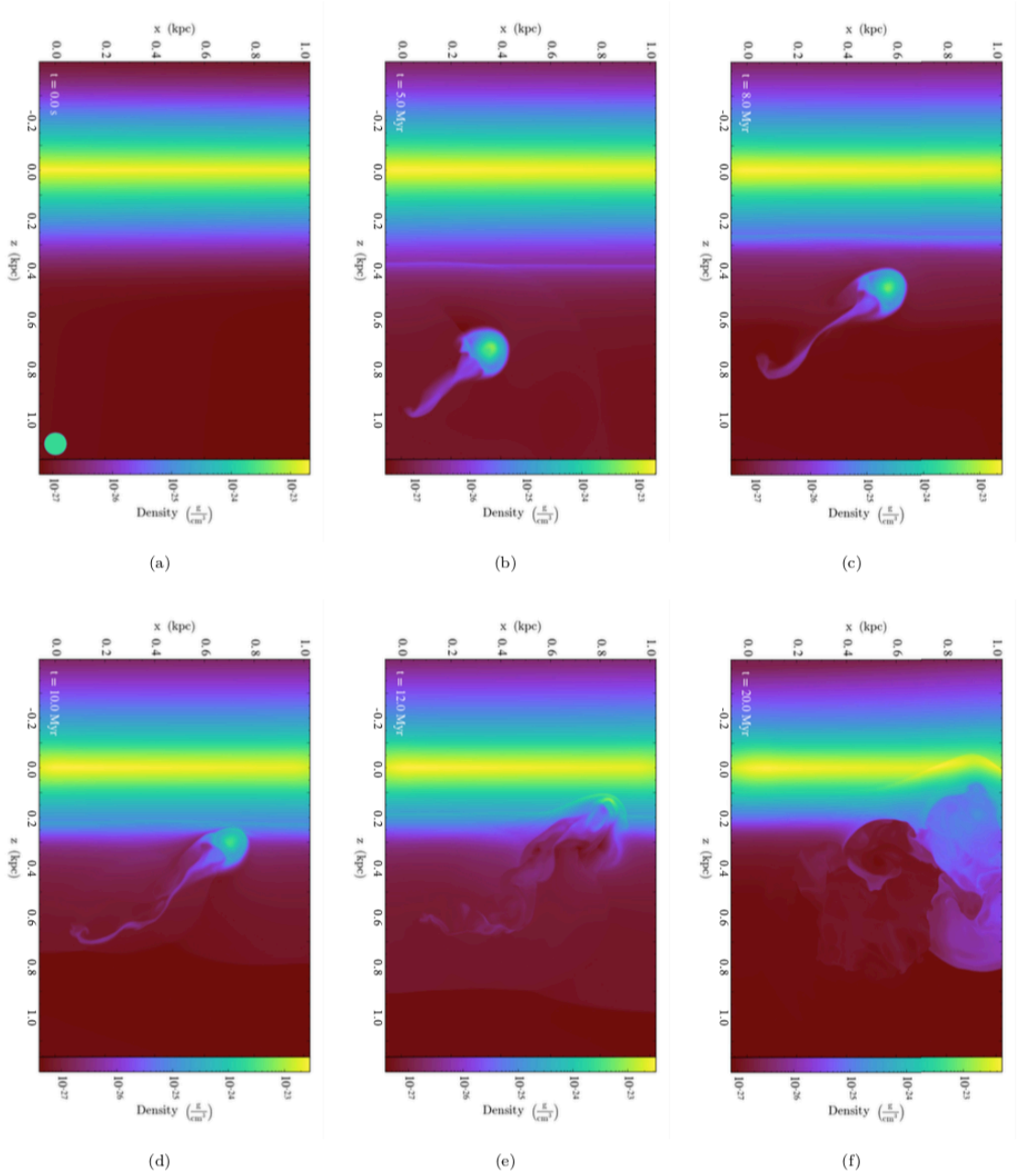

Figure 2. In the plots above, the evolution of the cloud can be seen from 0 to 20 Myrs for IVC 1 as it approaches the midplane, which is located at 0.0 kpc on the z-axis and crosses the domain horizontally. The initial cloud is seen in (a) before evolving over several epochs as seen in the following panels: (b) at 5.0 Myr, (c) at 8.0 Myr, (d) at 10.0 Myr, (e) at 12.0 Myr, and (f) at 20.0 Myr. These density plots represent a slice of the domain through the center of the cloud. The spherical cloud we begin with quickly forms a tail pointing away from the direction of motion. (f) shows the cloud will not survive its collision with the midplane but it will create a disturbance.

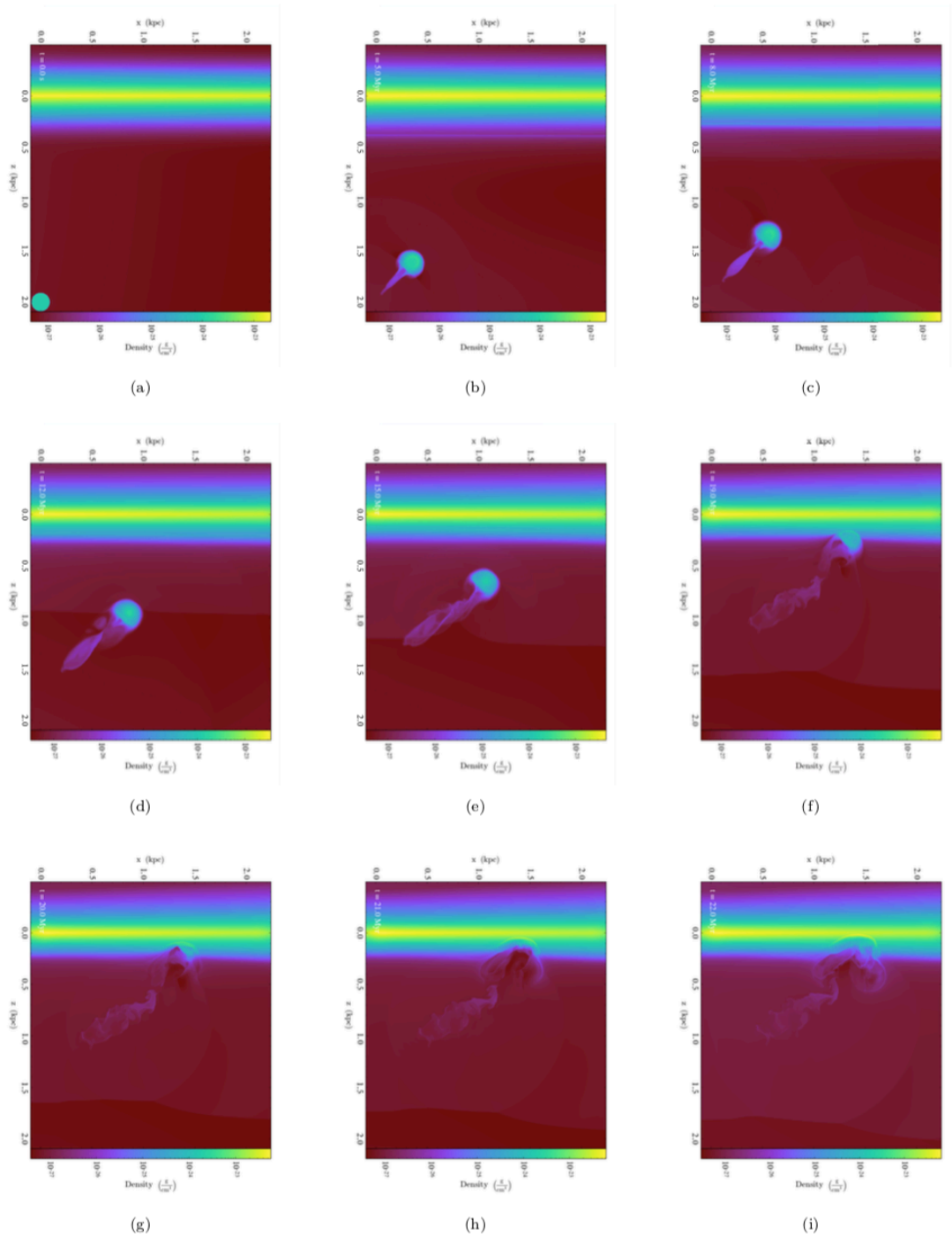

Figure 3. In the plots above, the evolution of the cloud can be seen from 0 to 22 Myrs for IVC 2. The initial cloud is seen in (a) before evolving over several epochs as seen in the following panels: (b) at 5.0 Myr, (c) at 8.0 Myr, (d) at 12.0 Myr, (e) at 15.0 Myr, (f) at 19.0 Myr, (g) at 20.0 Myr, (h) at 21.0 Myr, and (i) at 22.0 Myr. These density plots represent a slice of the domain through the center of the cloud. Beginning in (f), the head of the IVC is beginning to flatten as it enters a more dense region of the galactic disk. This flattening looks similar to the ridge seen in IVC 86-36.

2.3.2 Line-of-Sight Velocity

As seen in Figure 4, the line-of-sight (LOS) velocity for IVC 86-36 has a range between −40 and −70 km s^{-1}. The main portion of the head has a velocity of ∼−50 km s^{-1}. IVC 1 has a similar range of LOS velocities as IVC 86-36 but is moving slightly slower with velocities between ∼ −30 and −60 km s^{-1}. The main portion of the head of IVC 1, however, has a velocity that very closely matches that of IVC 86-36 at ∼ −50 km s^{-1}. In IVC 86-36, there is a long, straight portion of its tail that is moving faster than the rest of the cloud. It has a velocity between ∼ −60 and −70 km s^{-1}. Although it is not as clearly defined, there is a similar region in the tail of IVC 1 that has a velocity of ∼ −60 km s^{-1}. IVC 2 also has a range of velocities that is similar to that of IVC 86-36 between −30 and −70 km s^{-1}. The main portion of its head has a LOS velocity of ∼ −60 km s^{-1}. Each of the simulations have velocities that fit within the generally accepted range of IVC velocities, which is between 20 and 100 km s^{-1}.

2.3.3 Velocity Dispersion

In Figure 5, the velocity dispersion maps are shown for the head of IVC 86-36 and the two simulated clouds. Although IVC 86-36 is more mottled than the simulated clouds, the range of values do closely match. The HI in IVC 86-36 has a velocity dispersion range between 0 and 10 km s^{-1}. The range of velocity dispersion in the gas that has a temperature of 1×10^4 K or less in IVC 1 is between 0 and 12 km s^{-1}, while it is between 0 and 14 km s^{-1} for IVC 2. For IVC 86-36, there are several regions of note within its head. There is a long, straight ridge on the side of the head closest to the Galactic midplane. This region contains the greatest velocity dispersion at ∼ 8 km s^{-1}.

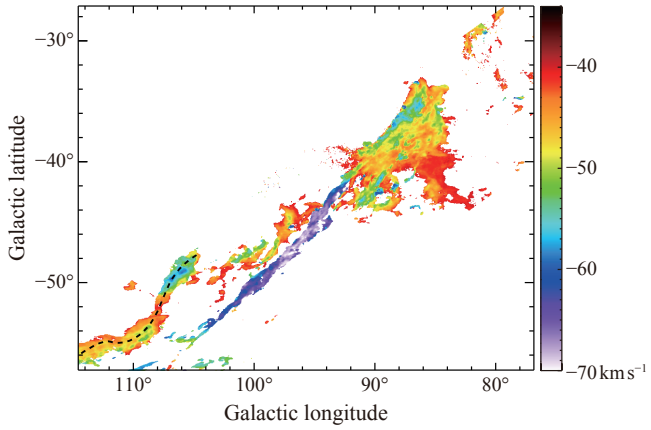

(a)

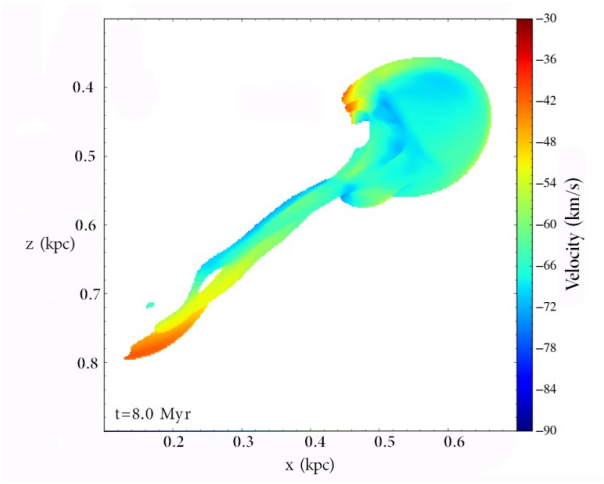

(b)

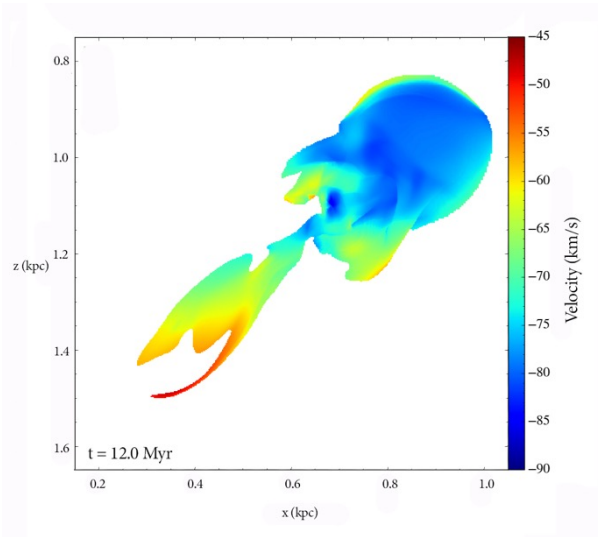

(c)

Figure 4. Line-of-sight velocity plots for (a) the observed cloud (IVC 86-36), (b) IVC 1 at 8.0 Myr, and (c) IVC 2 at 12.0 Myr. Each plot shows that the IVC undergoes a morphology similar to that of a comet with a clearly defined head and tail.

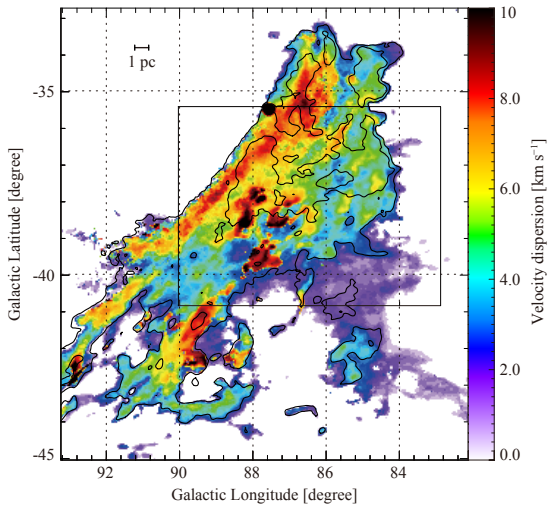

(a)

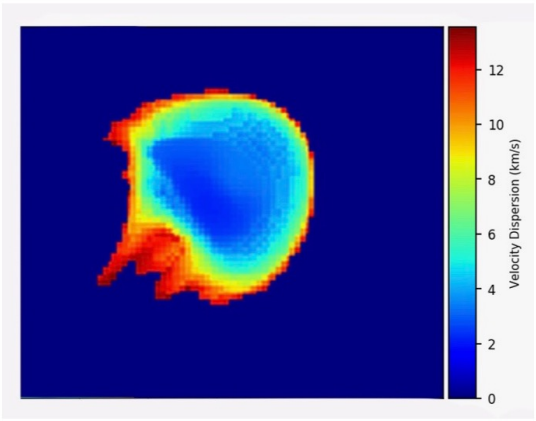

(b)

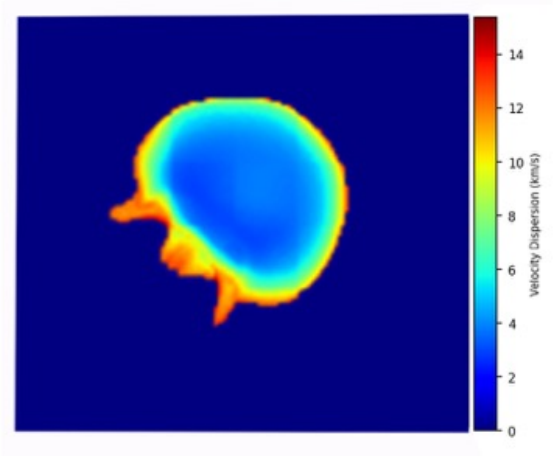

(c)

Figure 5. Velocity dispersion maps of the heads of (a) IVC 86-36, (b) IVC 1 at 8.0 Myr, and (c) IVC 2 at 12.0 Myr.

The other side of the head contains a region with the lowest velocity dispersion at about 1 km s^{-1}. In between these two sides is the main portion of the head of the cloud, which has a velocity dispersion ranging between ~4 and 6 km s^{-1}. This is the region that most closely matches the results of our simulations. Overall, the velocity dispersion of IVC 86-36 is slightly greater than that of the simulated clouds. This could indicate that IVC 86-36 has a higher temperature than the simulated clouds.

2.3.4 Intensity

Figure 6 shows the HI 21 cm intensity plots for IVC 86-36 and the two simulated IVCs. Assuming optically thin HI, the column density obtained from the simulations can be converted to HI 21 cm intensity by using the following formula:

$$I_{21\ cm} = \frac{N_H(cm^{-2})}{1.82 \times 10^{18}}$$

in which the units for intensity are K km s^{-1}. Looking toward the heads of the IVCs, the simulated clouds have similar HI 21 cm intensities as IVC 86-36. All of them have intensity ranges between ~ 0 and 200 K km s^{-1}. The intensity for each cloud is greatest at the head, as to be expected, due to that being the location with the greatest column density. For IVC 86-36, the main portion of the head has an intensity of ~ 100 K km s^{-1}, which is similar to that of the simulated clouds. However, IVC 86-36 does not show a smooth gradient from the center of the head out to the edges of the cloud like that seen in IVC 1 and IVC 2, which may require further analysis. Also, IVC 86-36 has a greater intensity throughout its tail which does not appear to exist in the simulated clouds.

(a)

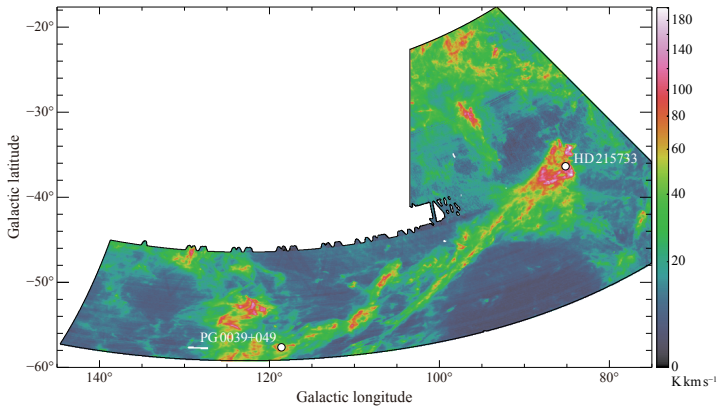

(b)

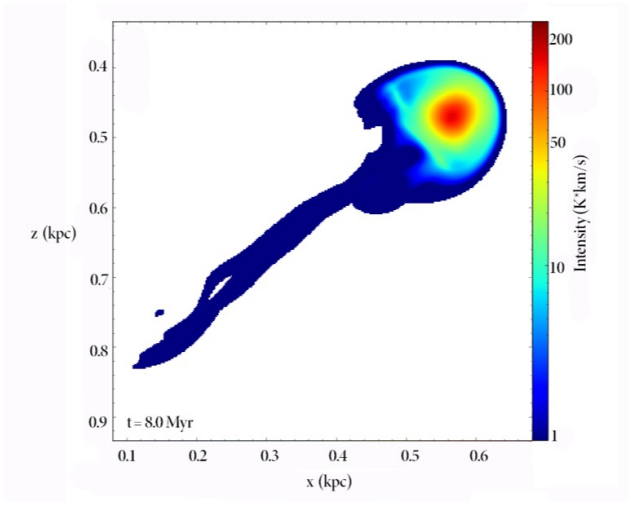

(c)

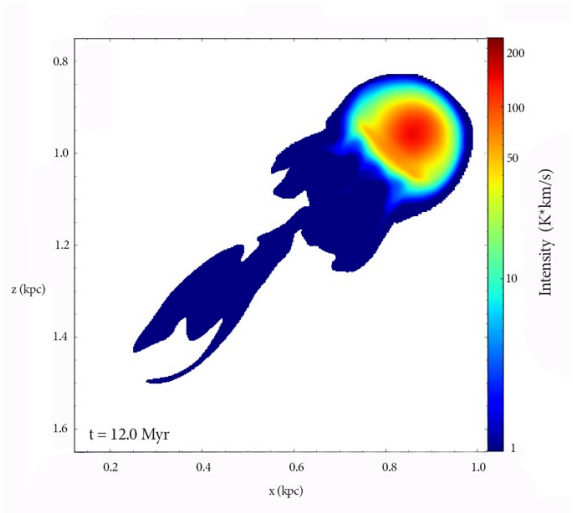

Figure 6. Intensity plots for (a) IVC 86-36, (b) IVC 1 at 8.0 Myr, and (c) IVC 2 at 12.0 Myr.

2.3.4 Predicting the Future for IVC 86-36

As seen in Figures 2(f) and 3(i), the simulated clouds do not survive the collision with the Galactic midplane. Although they make a significant disturbance within the disk, neither of them is capable of piercing the midplane and escaping to the other side. Based on these results, it does not seem likely IVC 86-36 will survive its inevitable collision with the Galactic plane. If this is the case, it may indicate that IVCs in general do not survive a cloud-disk collision, and, therefore, do not get recycled. In order for the Galaxy to continuously have IVCs, it must continuously produce them.

2.4 SUMMARY AND DISCUSSION

We have presented the results of hydrodynamic simulations of IVCs designed to match properties - angular size, mass, column density, etc. - of IVC 86-36 in the Pegasus-Pisces Arch. Our simulations began with a spherical cloud that was given a starting velocity within the range accepted for IVCs and allowed to evolve as the cloud approached and eventually collided with the Galactic midplane. In order to account for the uncertainty in the distance to IVC 86-36, two simulated models were created. Using the constraints Fukui et al. (2018) placed on the distance to the cloud, one models IVC 86-36 as if it is currently 200 pc from Earth, and the other models IVC 86-36 as if it is currently 3000 pc from the Earth. Based on the physical appearance and properties, IVC 86-36 most closely matches IVC 1. For instance, both IVC 86-36 and IVC 1 have long, straight tails, whereas, IVC 2 has a tail that is not as long in angular size or as straight. However, as seen in Figure 3(f), IVC 2 experiences the flattening of the side of its head that is closest to the Galactic midplane at a time greater than that seen in Figure 6(c). This

may indicate IVC 86-36 is on the lower end of the distance constraint at ~ 300 pc above the Galactic midplane. Another explanation for the flat ridge seen in IVC 86-36 could be a collision with another cloud we cannot see in the HI maps, such as an ionized cloud or a cloud whose velocity has shifted it out of the range observed by Fukui et al. However, this not accounted for in the current models.

There were also many other similarities between the simulated clouds and IVC 86-36 including cometary morphology, column density, intensity, velocity, and velocity dispersion. Both models produced the head-tail structure similar to that of a comet, which is also observed in IVCs as they interact with interstellar material. The HI 21 cm intensity range for the simulated clouds closely matches that of IVC 86-36. The LOS velocities for the models are not only within the acceptable range for IVCs, but they also very closely match the velocity of IVC 86-36. When comparing the velocity dispersion maps, IVC 86-36 has much more detail and is more mottled than the simulated clouds, but, overall, the velocity dispersion for all three clouds are very similar. Based on the results, it appears as though IVC 86-36 will not survive its inexorable impact with the Galactic plane. It will, however, cause a significant disturbance in the Galactic disk as the cloud begins to dissipate at ~ 300 pc above the midplane.

REFERENCES

Albert, C. E., & Danly, L. 2004, High Velocity Clouds, 312, 73

Blitz, L., Spergel, D. N., Teuben, P. J., & Hartmann, D. 1999, Stromlo Workshop on High-Velocity Clouds, 166, 125

Brüns, C., Kerp, J., Kalberla, P. M. W., & Mebold, U. 2000, A&A, 357, 120

Brüns, C., & Mebold, U. 2004, High Velocity Clouds, 312, 251

Connors, T. W., Kawata, D., Bailin, J., Tumlinson, J., & Gibson, B. K. 2006, ApJL, 646, L53

D'Onghia, E., & Fox, A. J. 2016, ARA&A, 54, 363

Fitzgerald, M.P., 1970, A&A, 4, 234

Fitzpatrick, E.L., Spitzer, L. 1997, ApJ, 475, 623

Fukui, Y., Koga, M., Maruyama, S., et al. 2018, PASJ

Fukui, Y., Tsuge, K., Sano, H., et al. 2017, PASJ, 69, L5

Galyardt, J., & Shelton, R. L. 2016, ApJL, 816, L18

Gritton, J. A., Shelton, R. L., & Kwak, K. 2014, ApJ, 795, 99

Heitsch, F., & Putman, M. E. 2009, ApJ, 698, 1485

Hernandez, A. K., Wakker, B. P., Benjamin, R. A., et al. 2013, ApJ, 777, 19

Kuntz, K. D., & Danly, L. 1996, ApJ, 457, 703

Lesh, J.R., 1968, ApJS, 17, 371

Lockman, F. J., Murphy, E. M., Petty-Powell, S., & Urick, V. J. 2002, ApJS, 140, 331

Magnani, L., & Smith, A. J. 2010, ApJ, 722, 1685

Mermilliod, J.-C., 1987, A&AS, 71, 119

Peek, J. E. G., Putman, M. E., McKee, C. F., Heiles, C., & Stanimirovic, S. 2007, ApJ, 656, 907

Richter, P., Wakker, B. P., Sembach, K. R., & Savage, B. D. 2001, Bulletin of the American Astronomical Society, 33, 11.09

Röhser, T., Kerp, J., Lenz, D., & Winkel, B. 2016, A&A, 596, A94

Tsuge, K., Sano, H., Tachihara, K., et al. 2019, ApJ, 871, 44

Wakker, B. P. 2001, ApJS, 136, 463

Wakker, B. P., & van Woerden, H. 1997, ARA&A, 35, 217

Walborn, N.R., 1976, ApJ, 205, 419